

# Dynamic Bridging Mechanisms of Through-Thickness Reinforced Composite Laminates in Mixed Mode Delamination

Hao Cui<sup>a,b,1</sup>, Mehdi Yasaei<sup>b</sup>, Stephen R. Hallett<sup>c</sup>, Ivana K. Partridge<sup>c</sup>, Giuliano Allegri<sup>d</sup>, Nik Petrinic<sup>a</sup>

<sup>a</sup>Department of Engineering Science, University of Oxford, Oxford, UK

<sup>b</sup>School of Aerospace, Transport and Manufacturing, Cranfield University, Cranfield, UK

<sup>c</sup>Advanced Composites Centre for Innovation and Science (ACCIS), University of Bristol, Bristol, UK

<sup>d</sup>Faculty of Aeronautics, Imperial College of London, London, UK

## Abstract

Delamination resistance of composite laminates can be improved with through-thickness reinforcement such as Z-pinning. This paper characterises the bridging response of individual carbon fibre/BMI Z-pins in mixed mode delamination at high loading rate using a split Hopkinson bar system. The unstable failure process in quasi-static tests, was also captured with high sampling rate instruments to obtain the complete bridging response. The energy dissipation of the Z-pins were analysed, and it was found that the efficacy of Z-pinning in resisting delamination growth decreased with an increase in mixed mode ratio, with a transition from pull-out to pin rupture occurring. The Z-pin efficacy decreased with loading rate for all mode mix ratios, due to the changing in failure surface with loading rate and rate-dependent frictional sliding.

**Keywords:** A. Fracture toughness; B. Failure; C. Delamination; D. 3-Dimensional reinforcement

---

<sup>1</sup> Corresponding author: email: [hao.cui@cranfield.ac.uk](mailto:hao.cui@cranfield.ac.uk);  
Phone: [+44\(0\)1234754494](tel:+44(0)1234754494)

## 1. Introduction

Longitudinal carbon fibre reinforced composite laminates have been applied in manufacturing primary aircraft structures [1] in the last decades and have also been used in other aerospace applications such as jet engine fan blades [2]. In design of these composite structures, foreign-object impact is one of the major concerns. The impact speed can range from less than 5 m/s in a drop weight event [3], up to more than 200 m/s during bird strike [4]. Due to the weak performance of epoxy matrix compared with that of reinforcement fibres and the lack of reinforcing fibres in the through-thickness direction, delamination is one of the dominating failure modes in these incidents [5, 6].

The delamination fracture toughness may be significantly improved with additional reinforcements in the through-thickness direction. The so called Z-pinning method has been invented as a cost-effective solution decades ago, metallic or carbon fibre rod are inserted in the through-thickness direction to improve the apparent fracture toughness [7, 8]. Standard fracture toughness experiments have been employed to measure the contribution of Z-pinning to the delamination toughness at quasi-static rates. The delamination toughness has been reported to increase with Z-pinning; in mode I delamination measured from the double cantilever beam (DCB) tests[8-10], mode II delamination measured from end notched flexure (ENF) tests[9] and mixed mode delamination measured from mixed-mode bending (MMB) tests[11]. It has also been shown that Z-pins are more effective in enhancing apparent fracture toughness for mode I delamination compared with mode II loading[12-14]. These experimental methods have been well-established for characterizing the delamination toughness in low loading rate; however, the complexity of their configuration and the considerable mass of the fixtures employed, make them quite challenging to be adopted in high loading rate systems such as a split Hopkinson bar apparatus. Schlueter used Z-pinned DCB samples loaded with flying wedge to investigate loading rates of up to 40m/s[15] and found a decrease in apparent

fracture toughness. The effect of Z-pinning in this test is however not straight forward to interpret due to the significant kinetic energy that dominates the fracture process[16]. Additionally, it is difficult to quantify the local loading rate near the Z-pin, as it may change significantly depending on the stability of the crack propagation. Cui et al. have thus developed a testing protocol that is suitable for use in a Hopkinson bar apparatus and is able to extract the rate dependent bridging response of an individual pin [17]. This was an evolution of the single pin test that has been used quasi-statically [9, 14, 18, 19], and was applied to pure mode I and pure mode II loading.

The bridging force that resists delamination growth with the relative displacement of delamination surfaces, the bridging response, is required for modelling of Z-pinned structural response[9, 20]. The response of Z-pins in mixed mode delamination has been characterized at quasi-static loading rates, and shows a transition of failure mode from pull-out to rupture as the mixed mode ratio increases[14, 21]. The high rate tests presented in [17] clearly showed the extremes of different behaviour under pure mode I and mode II loading, and showed that in particular the mode I behaviour was affected by the rate of loading. These tests [17] did not however cover the high rate behaviour of mixed mode cases in between the pure mode cases, which are more likely to be encountered in realistic loading of engineering structures. In particular, the transition between the high energy absorbing pull-out mode (mode I dominated) and the lower energy pin fracture mode (mode II dominated) is of interest at high loading rates.

The focus of this paper aims to develop a full understanding of the dynamic response of Z-pinned laminates under mixed mode loading. The experimental method developed for this work is introduced in Section 2. The bridging response, energy dissipation and failure mechanisms have been presented and discussed in Section 3. Brief outlining of conclusions out of this work can be found in Section 4.

## 2. Experiments

### 2.1. Specimen configuration

The direct measurement of single pin response in a dynamic test is a challenging proposal. There are three difficulties that must be addressed before a test method is designed. Firstly, the force to break or pull out a single pin is less than 50N and difficult to be accurately acquired with a split Hopkinson bar; Secondly, the complete failure displacement can be as large as half of the pin length in mode I dominated tests, and the striker will need to be long enough to ensure sufficient duration of the strain wave pulse; thirdly, the Z-pin failure may initiate at very small displacements at which point the equilibrium in the sample is not achieved. In the case of quasi-static tests, the Z-pins may fail in a very unstable manner in the mode II dominated tests, and the falling edge of the bridging-displacement curve is difficult to be captured. Given these challenges for the experimental characterization of Z-pin response, the specimen design and test configuration is introduced as follows.

IM7/8552 prepreg tapes from Hexcel were chosen for making the composite laminates, consistent with the material in [17]. A layer of PTFE film was inserted at the mid-plane of the laminates, to ensure that the measured bridging force was purely from the Z-pins. The layup in the top half was  $[0/45/90/-45]_{4S}$ , and the bottom half was  $[90/-45/0/45]_{4S}$ . This quasi-isotropic layup was chosen to represent the multi-directional laminates commonly used in industry, however the design ensured a  $90^\circ$  ply orientation mismatch at the centre-line to avoid fibre nesting. As shown in Fig.1, instead of a single pin (as for the quasi-static case in [14]) a 4x4 pin array was tested for each sample, to ensure the force response is large enough such that reliable measurement in the dynamic tests is achieved. The single pin performance was obtained as the average of these 16 pins. 0.28mm diameter pins made from T300/BMI were inserted with a pin to pin spacing of 1.75mm, representing a 2% volume fraction in practical

Z-pinned laminates. The Z-pin misalignment was checked for each sample, and the misalignment angles were found to be negligible.

The Z-pins were tested with different combinations of tension and shear loads using aluminium fixtures specially prepared for controlling the angle between the Z-pins and the loading axis, as illustrated in Fig.1. The Z-pinned samples were bonded to these fixtures with 3M Scotch-Weld DP490 adhesive. An M6 thread on one end of these fixtures was used to connect with the test machines. The off-axis angles,  $\beta$ , that the specimens were tested at were  $0^\circ$ ,  $15^\circ$ ,  $30^\circ$ ,  $45^\circ$ ,  $60^\circ$  and  $75^\circ$ , giving a gradual transition from pure mode I to shear dominated delamination failure in mode II. A brass sleeve was used in the mixed mode tests, to prevent the rotation and lateral displacement of the aluminium fixtures.

## **2.2. Test setup**

Quasi-static tests were conducted at the loading rate of 0.01 mm/s using a Zwick Roell 250 test machine. As sketched in Fig.2, A USB camera was used to record the test at frame rate of 1 FPS, and the load was monitored with the loading cell on Zwick machine. A thin aluminium tube was attached between the specimen and the loading cell. A strain gauge attached on the tube was connected to a strain signal conditioner and ultra-high frequency oscilloscope, used for capturing the loading signal in the event of unstable failure. The tube was 0.9m long; ensuring that the entire falling edge of the bridging force could be measured before the reflected wave from the loading cell end reached the strain gauge. An Ultra-high speed SI-Kirana camera was triggered by the oscilloscope once the force started to drop, and the deformation of samples during unstable damage was recorded at frame rate of 200,000 FPS.

A split Hopkinson tension bar was used in dynamic tests [22]. As shown in Fig.2, the projectile was accelerated to strike a stopper at the end of the loading bar, providing a tension stress pulse with duration of 1ms. The stress pulse passed through the input bar, and applied a

tensile load to the samples. The stress pulse transmitted through the sample was recorded using a strain gauge on the output bar. Using the input and transmitted strain waves, the force on the samples could be estimated. The SI-Kirana camera was used for recording the deformation of the samples at frame rate of 100,000 – 500,000 FPS, depending on the duration of the failure event.

The specimen surface was painted with black speckles on a white back ground. The digital image correlation (DIC) method was used to track the open and shear displacement of the specimen (in-house [23] and commercial software GOM Aramis were used)..

### 2.3. Data processing

The applied displacement in the global system was converted to shear and opening relative displacements of the specimen mid-plane surfaces as follows:

$$\delta_s = D_x \sin(\beta + \chi) - D_y \cos(\beta + \chi) \quad (1a)$$

$$\delta_T = D_x \cos(\beta + \chi) + D_y \sin(\beta + \chi) \quad (1b)$$

$$\delta_M = \sqrt{\delta_s^2 + \delta_T^2} \quad (1c)$$

where  $D_X$  and  $D_Y$  are the relative displacement between the two pre-delaminated laminates of the specimen,  $\delta_s$  is the relative shear displacement,  $\delta_T$  the relative tension displacement and  $\delta_M$  the mixed mode relative displacement.  $\chi$  is the additional rotation of the Z-pins due to the gap between aluminium fixture and brass sleeve.

The strain gauge used on the aluminium tube in quasi-static tests, and these attached on the split Hopkinson bars were calibrated prior to experiments. The force applied on the sample can be calculated as:

$$P = \varepsilon C_f \quad (2)$$

where  $\varepsilon$  is the tensile strain of the bar measured with strain gauge and  $C_f$  is the calibration factor between force and the strain. In dynamic tests, the bridging force was also calculated with Eq (2) using the strain signal on the output bar.

In dynamic tests, the samples were accelerated to the desired velocity within a very short period. It is possible that the stress equilibrium within the samples and the aluminium fixtures may not be reached before the damage initiation. The inertia force due to the mass of the aluminium fixture and specimen therefore needs to be corrected from the measured force using bar signals. The acceleration of the specimen can be estimated using the displacement from DIC, knowing the time interval between each frame. The actual force on the samples was corrected as:

$$F = P - F_1 \quad (3)$$

where the inertia force is:

$$F_1 = mA \quad (4)$$

and  $m$  is the mass of the aluminium fixture and half of the specimen,  $A$  is the acceleration value determined from the DIC.

In quasi-static tests, the failure process tends to be unstable, especially for shear dominated delamination cases. The strain gauge on the aluminium tube was used to capture the falling edge of the bridging response. The sample was accelerated during this unstable failure process, due to the stored elastic energy in the sample and the attached aluminium tube. This inertia effect from the aluminium fixture and laminates, caused an overestimation of the bridging force in unstable failure, and should be corrected. In this work, the acceleration of the

laminates and fixture was obtained from the images taken by the Kirana camera using DIC methods, and Eq (3, 4) were used to get the correct bridging force at the falling edge.

### **3. Results and discussion**

#### **3.1. Failure process**

The failure process recorded with the Kirana high-speed video camera in the dynamic tests is shown in Fig.4 for representative results corresponding to mode I and mode II dominated failure. The completed failure was reached when the bridging force vanished to zero as determined from the Hopkinson bar signal. The Z-pins failed at much smaller displacement when loaded predominately in shear than in tension. Detailed discussion on the failure mechanisms is given in Section 3.6. The relative displacement of each half of the laminates was analysed using DIC and is given as follows.

The relative opening and shear displacements (illustrated in Fig.3) that the Z-pinned specimens' mid-plane experienced before complete failure is plotted in Fig.5. The displacement at damage initiation illustrated in the dashed boxed in Fig.5a and c, are plotted enlarged in Fig.5 b and d. The solid lines represent the displacement from images recorded with high speed camera, and the dash-dot lines represent the values from USB camera images. Despite the constraint from brass sleeve in the mixed mode tests, the shear to tension displacement ratios were not constant during the tests. This might be due to there being a small gap between the aluminium fixture and brass sleeve, as tolerances within the scale of dozens of microns were unavoidable in the manufacturing process. Additionally, the traction from the Z-pins tend to close the delamination surfaces, and also cause the initially higher shear to opening displacement ratio. The ratios became closer to the nominal values as the displacement increased. Similar trends were found in both quasi-static and dynamic tests. Due to the



relatively small displacement in shear dominated tests ( $\beta=60^\circ, 75^\circ$ ), the shear to opening displacement ratios didn't converge to the nominal values, even at final failure.

### **3.2. Bridging response**

The bridging force experienced a very rapid drop in quasi-static tests, due to either the debonding between Z-pin and matrix, or the unstable rupture of Z-pins. The high-speed camera was triggered by the sharp drop of bridging force to record the unstable failure process. The displacement of the laminates connected with the aluminium fixture was then obtained with DIC method, which increased rapidly at the moment of damage initiation as shown in Fig.6a. The velocity increased at an almost linear rate until about 1.2 m/s. The falling edge of the bridging force in quasi-static tests was monitored by the strain gauge mounted on the aluminium tube, with high frequency data acquisition systems. This was then corrected by considering the inertia effect due to the acceleration of the aluminium block and laminates. As shown in Fig.6b, the complete bridging response in quasi-static tests were comprised of the force from the loading cell and the aluminium tube, and the displacements were determined from images taken by the USB and the Kirana cameras.

The existence of this aluminium tube as a force measurement instrument may influence the failure process in quasi-static tests, as the release of the stored elastic energy may promote unstable failure of the pins, and bring in dynamic effect. Experiments without this tube were also carried out on samples with low mode mix angle, as a reasonably complete bridging response can be captured with low sampling rate instruments in this particular case. As shown in Fig.7, the jump of displacement was much smaller without the bar, but the influence was limited to less than 0.4mm, much smaller than the overall displacement for complete failure. In the shear dominated failure mode, the fracture was unstable even without the bar, and the bar measurements became vital to capture the falling edge of the bridging force. The unstable

failure processes were captured by the bar in quasi-static tests, but they were not anymore quasi-static fracture events from the aspect of local deformation rate. It can be seen from Fig.6a that the corresponding velocity at the unstable failure process was even comparable with that in dynamic tests.

In the dynamic tests, the Z-pinned samples were pulled in the bar direction, due to the tension stress pulse. The longitudinal displacement of both sides of the laminates near the input bar and output bar are plotted in Fig.8a for one representative test. The mixed mode displacement of the Z-pins increased nonlinearly, and then a relatively constant velocity was reached after about the first 1 mm. No equilibrium was reached before the initiation of damage in these dynamic tests due to the mass and geometry of the samples, the force measured by the output bar thus needs to be corrected for the inertia effect. As shown in Fig.8b, the inertia force was noticeable in the beginning, and vanished as the displacement increased. All dynamic test results have been corrected with consideration of inertia effects in this study[17], and will be presented in the next section.

The single pin response, as averaged from 16 pins for each sample, is plotted in Fig.9. Thanks to the relatively large number of pins tested for each sample, the experimental results showed very good repeatability and low scatter. In the pure mode I case, the bridging force increased to its maximum within very small displacement, followed by a sharp drop due to the interfacial failure between the Z-pin and the laminates. The bridging force increased again despite the fact that the length of Z-pins supplying frictional stress decreased. No enhanced friction zone exists in pure mode I tests as the pin misalignment was negligible in these laminates[17]. This nonlinear increase of bridging force may be attributed to the evolution of the frictional interface with sliding[24]. The bridging force in dynamic tests decreased almost linearly with the displacement.

The maximum force was around 40N for all tests, and no dependence on the loading rate or mode mix ratio was noticed. For the tests with low mode mix ratio ( $\beta = 15^\circ$  and  $30^\circ$ ), there were distinct steps in the bridging force after debonding in quasi-static tests, probably due to the rupture of individual pins. The bridging force increased nonlinearly within the first 1mm, and then decreased linearly until the complete pulling-out in dynamic tests. The displacement at complete failure of Z-pins decreased significantly when mode mix angle was higher than  $45^\circ$ , and it decreased with the loading rate.

### 3.3. Energy dissipation

The Z-pins were efficient in improving the apparent delamination toughness of laminates composites, because of the energy dissipated during the failure or pull-out of the pins. In this study, the energy dissipation was calculated by integrating the area under the bridging curve, and is summarized in Fig.10. Pure mode I tension and mode II shear dynamic tests on Z-pins have been done previously [17] with the mixed mode angles corrected to include the pin misalignments and these data have also been included in Fig.10. The increase in energy dissipation in the pure mode II static case was thought to be due to friction at the delaminated interface rather than due to pin failure (see [17] for details). The energy dissipation increased first, and reached its maximum at a mixed mode angle of about  $9^\circ$ . This increase of Z-pin efficacy was mainly caused by the bending deformation Z-pins, as the lateral pin displacement introduced compressive stress onto surrounding laminates, and resulted in the enhanced friction force at low mixed mode angle [25, 26]. With further increase in mode mix angle, the energy dissipation decreased monotonically. This is caused by the change in failure mode, as will be discussed in Section 3.4. The composite laminates with a single pin was tested at quasi-static rate by Yasaei et.al [14], and the energy dissipation over the full range of mode mixities is plotted in Fig.10. The generic trends agreed nicely with the quasi-static results obtained in this work, despite the noticeable scatters from single pin tests. The dynamic tests provided lower

energy dissipation than quasi-static tests in all mode mix ratios, and it can be concluded that the Z-pinning efficiency in improving the delamination resistance decreases with loading rate. The strain rate effect on the energy dissipation was more significant for lower mode mix ratio.

### **3.4. Failure mechanisms**

The Z-pin failure mode changed considerably with the mode mix ratio. All pins were pulled out in the pure mode I case ( $\beta = 0^\circ$ ), similar to reported in literatures [14, 18, 19]. The representative failure processes for mixed mode failure were analysed with scanning electron microscopy as shown in Fig.11. Some Z-pins were pulled out completely from the laminates at low mixed mode ratios when  $\beta$  is equal to  $15^\circ$  and  $30^\circ$ . Longitudinal splits extended along the whole length of the Z-pins in the quasi-static tests, while in dynamic tests this damage was observed around the mid-plane only. From this evidence it can be postulated that the difference at varied loading rates is due to the inertia effect of the Z-pins and the enhanced inter-fibre shear strength at high strain rate[27]. The longitudinal splits will cause a decrease in the Z-pin bending stiffness. This may help to delay the pin rupturing due to the pin becoming more compliant and reducing the peak fibre tensile stresses endured. A numerical study in [28] showed that Z-pins with lower splitting density demonstrate a more brittle behaviour while Z-pins with higher splitting density offer a more ductile behaviour. Higher levels of splitting will however hinder the presence of enhanced friction zone in these tests, and could be partially responsible for the decrease of Z-pin efficacy when  $\beta$  is larger than  $9^\circ$ . Some broken Z-pins were also present, with a considerable length of these Z-pins being pulled out. There were no Z-pins being pulled out completely when the mixed mode angle  $\beta$  is  $45^\circ$  or above. As shown in Fig.11c and d, the Z-pin ruptured at the position a few hundred microns from the mid-plane. The Z-pins were split in quasi-static tests, while no significant splitting was found in dynamic test samples. With the increase in mixed mode ratio, the Z-pins were ruptured at a position closer to the mid-plane, leading to lower pull-out lengths [29]. The energy dissipation during

the failure of Z-pins decreased with mode mix ratio, mainly due to the pin rupture and reduced energy dissipation during frictional pull-out stage.

The difference between dynamic and quasi-static response was much more significant in pull-out dominated failure than that in shear dominated cases. This may be attributed to the rate dependence of the friction and interface properties during the pull-out process, which was studied analytically and numerically at the fibre level by Liu et.al[30, 31]. By contrast the fibre failure dominated rupture of Z-pins was generally not very rate sensitive.

Two 15° samples (static and dynamic) were polished back to the remaining hole after the Z-pins were pulled out for SEM analysis. The section at the mid-length of the hole is presented in Fig.12, which reveals the influence of frictional sliding between the laminate and the Z-pin. Shear cusps are visible due to the shear dominated failure process. Considerable abrasion marks were also noticed on the failure surface, as some shear cusps have been almost rubbed off, leaving a smooth imprint from the sliding of carbon fibres. In the dynamic tests, the shear cusps were smaller in size, and the fracture surface was less rough than that in quasi-static tests, as shown in Fig.12. This is consistent with SEM evidence of the effect of rate on the fracture surface morphology in [27] where  $\pm 45^\circ$  in-plane shear tests were conducted. The fracture morphology here also showed a dependence on the loading rate, with the rougher frictional interface in quasi-static testing being able to help increase the Z-pining efficacy in pull-out.

## **4. Conclusions**

The dynamic response of Z-pins was tested in different combinations of tension and shear displacement for the first time. The study aimed at a fundamental investigation of rate effects on the pin-laminate interaction that are a necessary part of understanding and interpreting larger scale coupon or structural tests, that will be the subject of future work. In

fracture tests such as DCB/ENF/MMB it is not possible to control the pin deformation precisely. Any detailed analysis of pin behaviour is therefore smeared out in the global response. Here it has been shown that the Z-pin efficacy in improving the delamination resistance decreased with the increase of mode mix ratio, which was attributed to the transition from pull-out to rupture failure and the decreased length of Z-pins being fictionally pulled out. The Z-pin efficacy in dynamic tests has been found to be lower than that in quasi-static tests for the loading rates studied here, and the difference was more significant in mode I dominated delamination than that in mode II dominated cases.

The change in Z-pinning behaviour mainly came from the change of fracture morphology with loading rate, with the rough surface in quasi-static tests provided more frictional bridging force than that in dynamic tests. This study suggested that, the strain rate effect needs to be considered in the design and analysis of through-thickness reinforced composites threatened by impact loading, as quasi-static experiments and analysis may overestimate the Z-pin efficacy.

## **5. Acknowledgement**

This research was supported by EPSRC funding in the UK (grant no EP/M012905/1).

The research data are available at [URL to be inserted after review]

## **6. References**

[1] Fawcett AJ, Oakes GD. Boeing Transport Experience with Composite Damage Tolerance & Maintenance. In: Research NIfA, editor. FAA workshop for composite damage tolerance and maintenance. CHICAGO2006. p. 32.

[2] Miller SG, Handschuh KM, Sinnott MJ, Kohlman LW, Roberts GD, Martin RE, et al. Materials, Manufacturing, and Test Development of a Composite Fan Blade Leading Edge Subcomponent for Improved Impact Resistance. NASA/TM—2015-218340. Cleveland, Ohio: Glenn Research Center, NASA; 2015.

[3] Aslan Z, Karakuzu R, Okutan B. The response of laminated composite plates under low-velocity impact loading. *Composite Structures*. 2003;59:9.

[4] Nishikawa M, Hemmi K, Takeda N. Finite-element simulation for modeling composite plates subjected to soft-body, high-velocity impact for application to bird-strike problem of composite fan blades. *Composite Structures*. 2011;93(5):1416-23.

[5] Johnson AF, Holzapfel M. Modelling soft body impact on composite structures. *Composite Structures*. 2003;61(1-2):103-13.

[6] Morita H, Tsang PHW. Soft Body Impact Damage on CF/PEEK Laminates using Gelatin Projectile. *Journal of Reinforced Plastics and Composites*. 1997;16:12.

[7] Mouritz AP. Review of z-pinned composite laminates. *Composites Part A: Applied Science and Manufacturing*. 2007;38(12):2383-97.

[8] Partridge IK, Cartié DDR. Delamination resistant laminates by Z-Fiber® pinning: Part I manufacture and fracture performance. *Composites Part A: Applied Science and Manufacturing*. 2005;36(1):55-64.

[9] Cartié DDR, Troulis M, Partridge IK. Delamination of Z-pinned carbon fibre reinforced laminates. *Composites Science and Technology*. 2006;66(6):855-61.

[10] Byrd LW, Birman V. Effectiveness of z-pins in preventing delamination of co-cured composite joints on the example of a double cantilever test. *Composites Part B: Engineering*. 2006;37(4-5):365-78.

[11] Rugg KL, Cox BN, Massabo R. Mixed mode delamination of polymer composite laminates reinforced through the thickness by Z-fibers. *Composites Part A: Applied Science and Manufacturing*. 2002;33.

[12] Pegorin F, Pingkarawat K, Daynes S, Mouritz AP. Influence of z-pin length on the delamination fracture toughness and fatigue resistance of pinned composites. *Composites Part B: Engineering*. 2015;78:298-307.

[13] M'Membe B, Gannon S, Yasaee M, Hallett SR, Partridge IK. Mode II delamination resistance of composites reinforced with inclined Z-pins. *Mater Design*. 2016;94:565-72.

[14] Yasaee M, Lander JK, Allegri G, Hallett SR. Experimental characterisation of mixed mode traction–displacement relationships for a single carbon composite Z-pin. *Composites Science and Technology*. 2014;94:123-31.

[15] Schlueter AM. An Experimental Study of Rate Effects on Mode I Delamination of Z-pinned Composite. West Lafayette: Purdue University; 2012.

[16] Sridhar N, Massabo R, Cox BN, Beyerlein IJ. Delamination dynamics in through-thickness reinforced laminates with application to DCB specimen. *International Journal of Fracture*. 2002;118:26.

[17] Cui H, Yasaee M, Kalwak G, Pellegrino A, Partridge IK, Hallett SR, et al. Bridging mechanisms of through-thickness reinforcement in dynamic mode I&II delamination. *Composites Part A: Applied Science and Manufacturing*. 2017;99:198-207.



- [18] Dai S-C, Yan W, Liu H-Y, Mai Y-W. Experimental study on z-pin bridging law by pullout test. *Composites Science and Technology*. 2004;64(16):2451-7.
- [19] Liu H, Yan W, Yu X, Mai Y. Experimental study on effect of loading rate on mode I delamination of z-pin reinforced laminates. *Composites Science and Technology*. 2007;67(7-8):1294-301.
- [20] Cui H, Li Y, Koussios S, Beukers A. Mixed mode cohesive law for Z-pinned composite analyses. *Comp Mater Sci*. 2013;75:60-8.
- [21] Pegorin F, Pingkarawat K, Mouritz AP. Mixed-mode I/II delamination fatigue strengthening of polymer composites using z-pins. *Composites Part B: Engineering*. 2017;123:219-26.
- [22] Gerlach R, Kettenbeil C, Petrinic N. A new split Hopkinson tensile bar design. *Int J Impact Eng*. 2012;50:63-7.
- [23] Jumpasut A, Petrinic N, Elliott BCF, Siviour CR, Arthington MR. An Error Analysis into the Use of Regular Targets and Target Detection in Image Analysis for Impact Engineering. *Applied Mechanics and Materials*. 2008;13-14:203-10.
- [24] Yasaee M, Bigg L, Mohamed G, Hallett SR. Influence of Z-pin embedded length on the interlaminar traction response of multi-directional composite laminates. *Composites Part A: Applied Science and Manufacturing*. 2016;Submitted
- [25] Cox BN. Snubbing effects in the pullout of a fibrous rod from a laminate. *Mech Adv Mater Struc*. 2005;12(2):85-98.
- [26] Cui H, Li Y, Koussios S, Zu L, Beukers A. Bridging micromechanisms of Z-pin in mixed mode delamination. *Composite Structures*. 2011;93(11):11.

- [27] Cui H, Thomson D, Pellegrino A, Wiegand J, Petrinic N. Effect of strain rate and fibre rotation on the in-plane shear response of  $\pm 45^\circ$  laminates in tension and compression tests. *Composites Science and Technology*. 2016;135:106-15.
- [28] Zhang B, Allegri G, Yasaee M, Hallett SR. Micro-mechanical finite element analysis of Z-pins under mixed-mode loading. *Composites Part A: Applied Science and Manufacturing*. 2015;78:424-35.
- [29] Yasaee M, Mohamed G, Pellegrino A, Petrinic N, Hallett SR. Strain rate dependence of mode II delamination resistance in through thickness reinforced laminated composites. *Int J Impact Eng*. 2017;107:1-11.
- [30] Liu H-Y; Zhang X, Mai Y-W, Diao X-X. On steady-state fibre pull-out II: Computer simulation. *Composites Science and Technology*. 1999;59.
- [31] Zhang X, Liu H-Y, Mai Y-W, Diao X-X. On steady-state fibre pull-out I The stress field. *Composites Science and Technology*. 1999;59:11.

## Figures

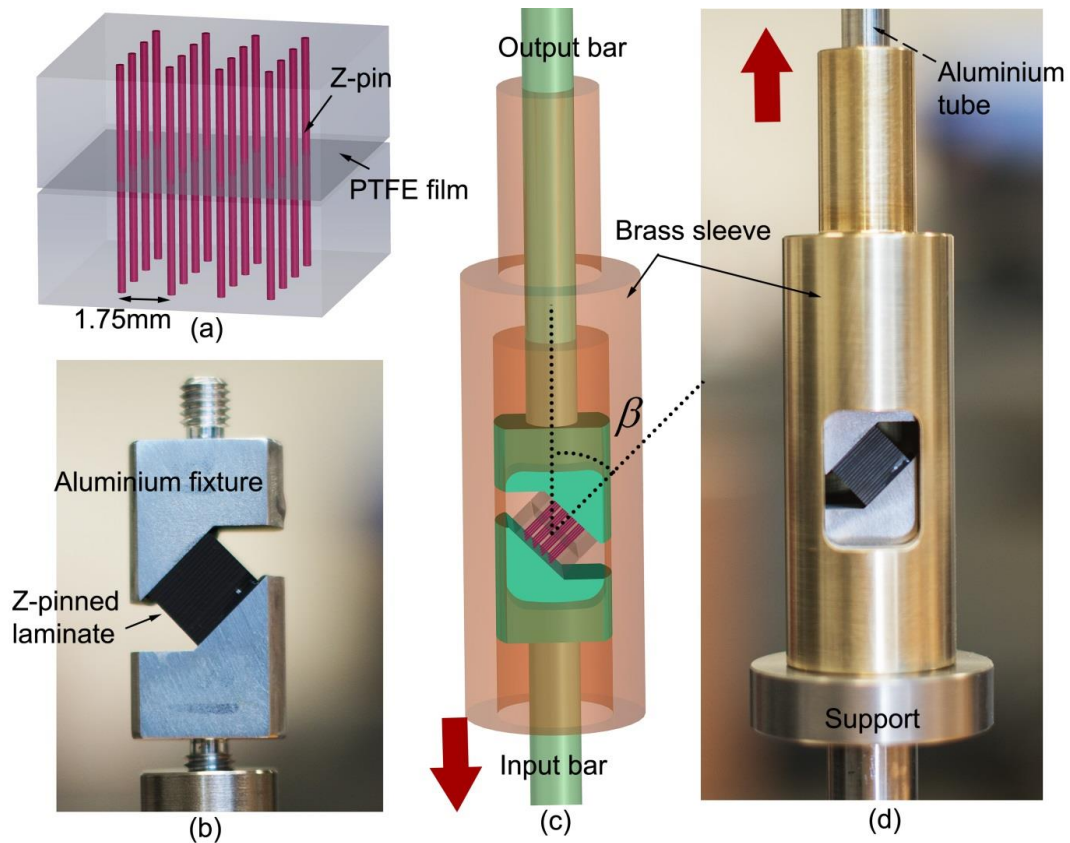


Fig.1 (a) Z-pin array within the laminates; (b) the aluminium fixture; (c) lateral constraint in dynamic tests; (d) quasi-static configuration

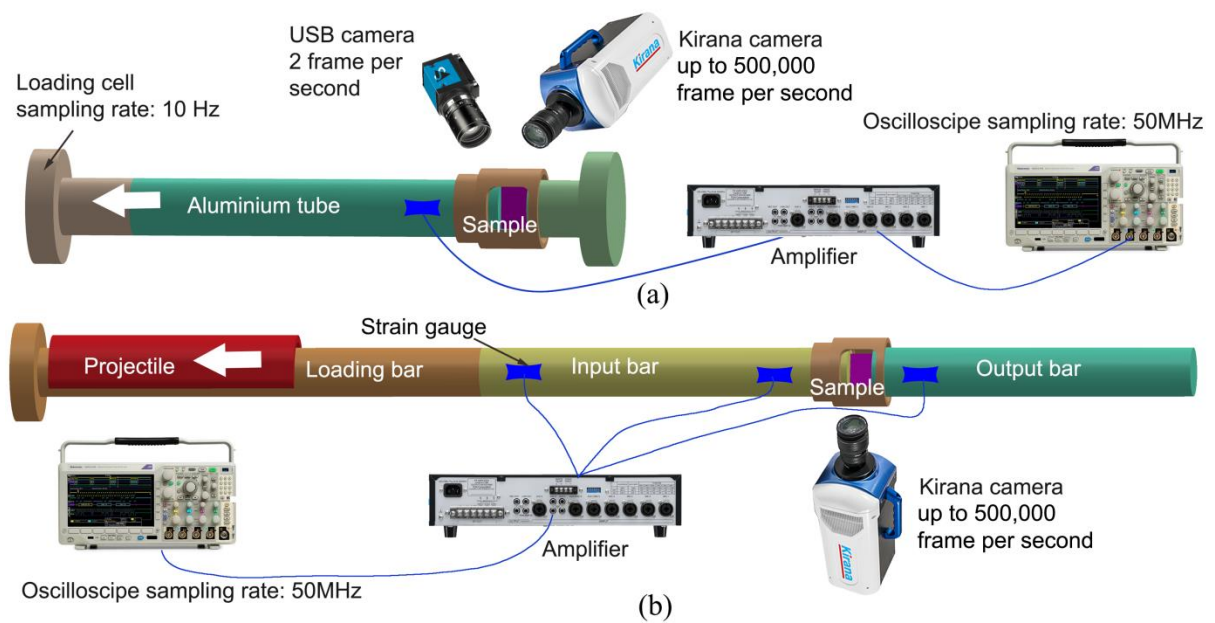


Fig.2 The complete experimental setup for (a) quasi-static and (b) dynamic tests

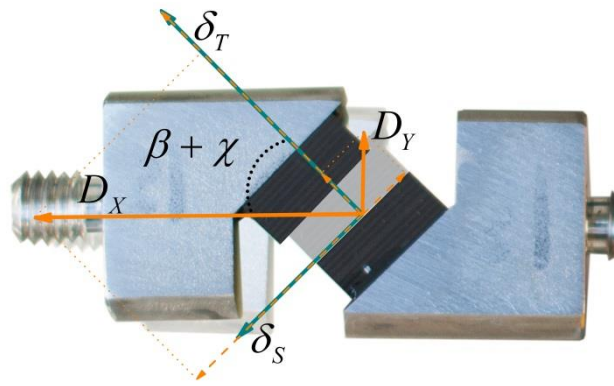


Fig.3 Calculation of the tension and shear displacements

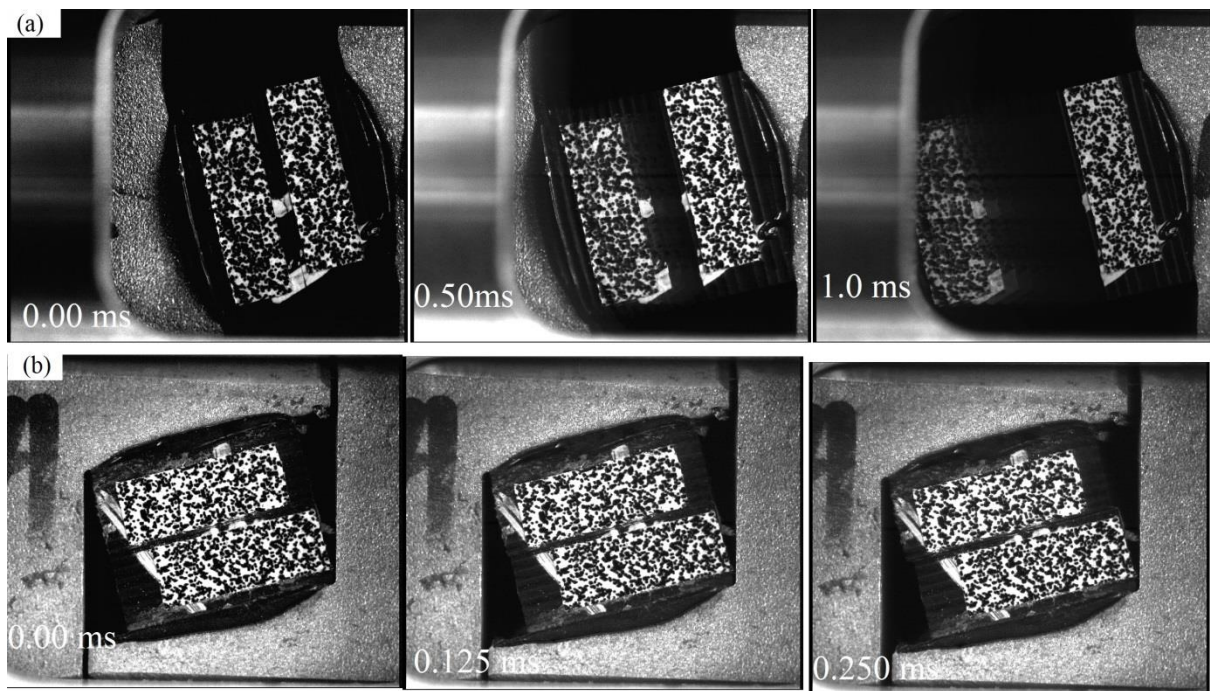


Fig.4. Dynamic failure process in mixed mode failure (a)  $\beta = 15^\circ$ ; (b)  $\beta = 75^\circ$

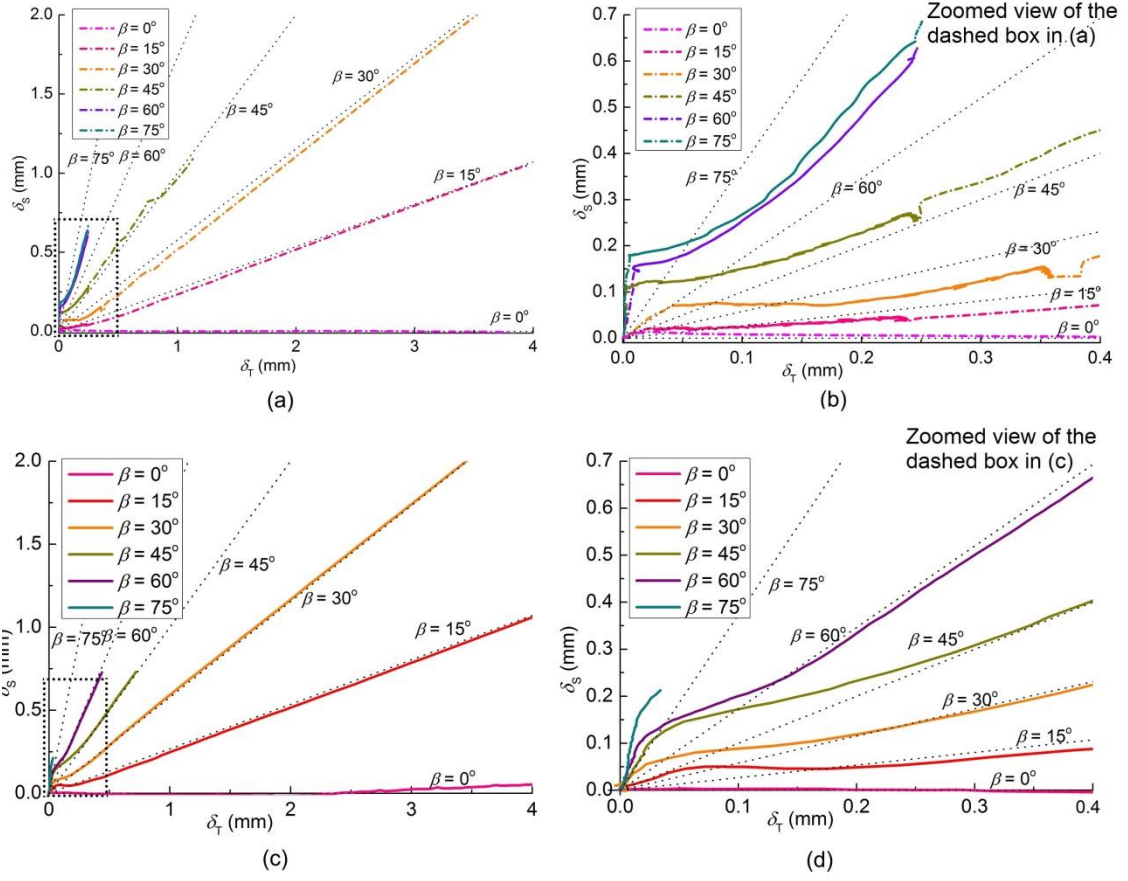


Fig.5. Tension-shear relative displacement ratio at different mode mix angle, (a, b) quasi-static tests; (c, d) dynamic tests

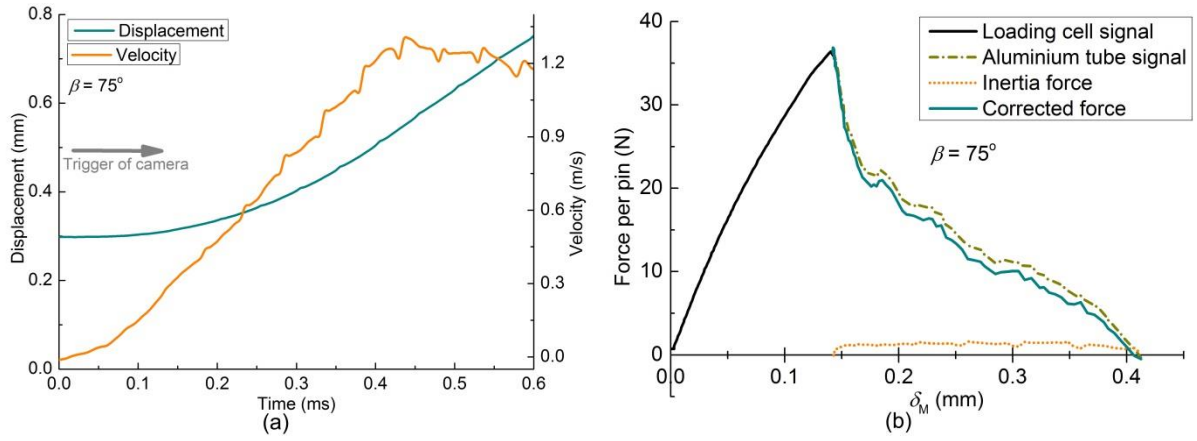


Fig.6. Quasi-static test results when  $\beta=75^\circ$ : (a) displacement and velocity captured with high-speed camera at the event of unstable failure; (b) the complete bridging response with correction of inertia effect

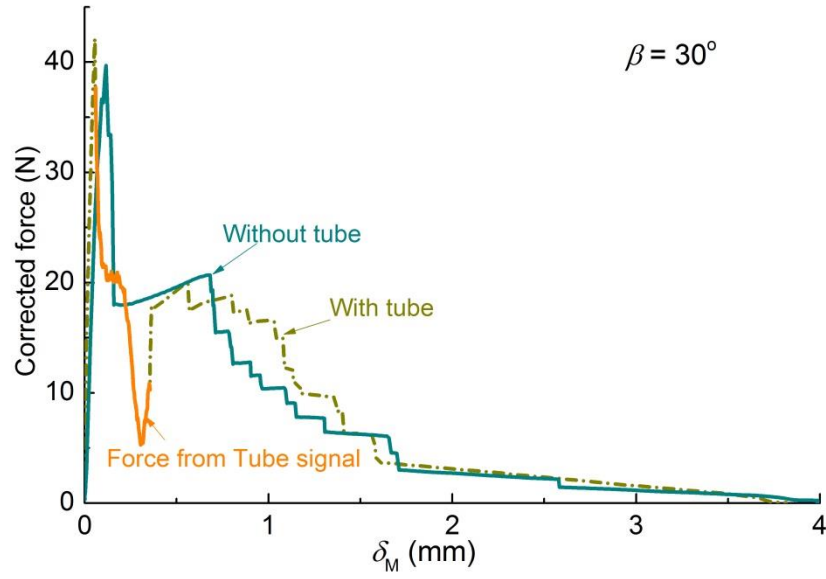


Fig.7. Influence of the aluminium tube on the Z-pin bridging response

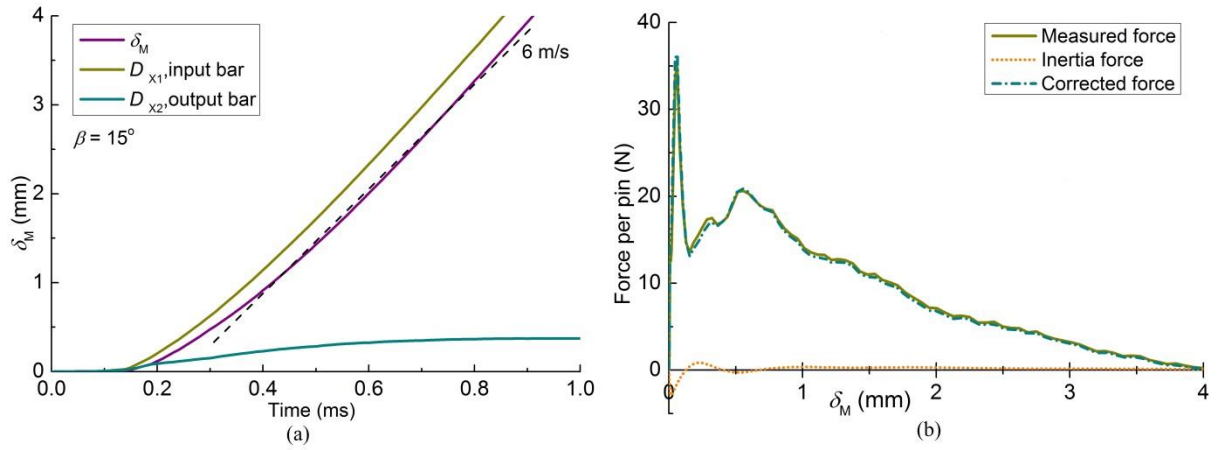


Fig.8 (a) displacement of the sample and the end of the bars; (b) force-displacement curve



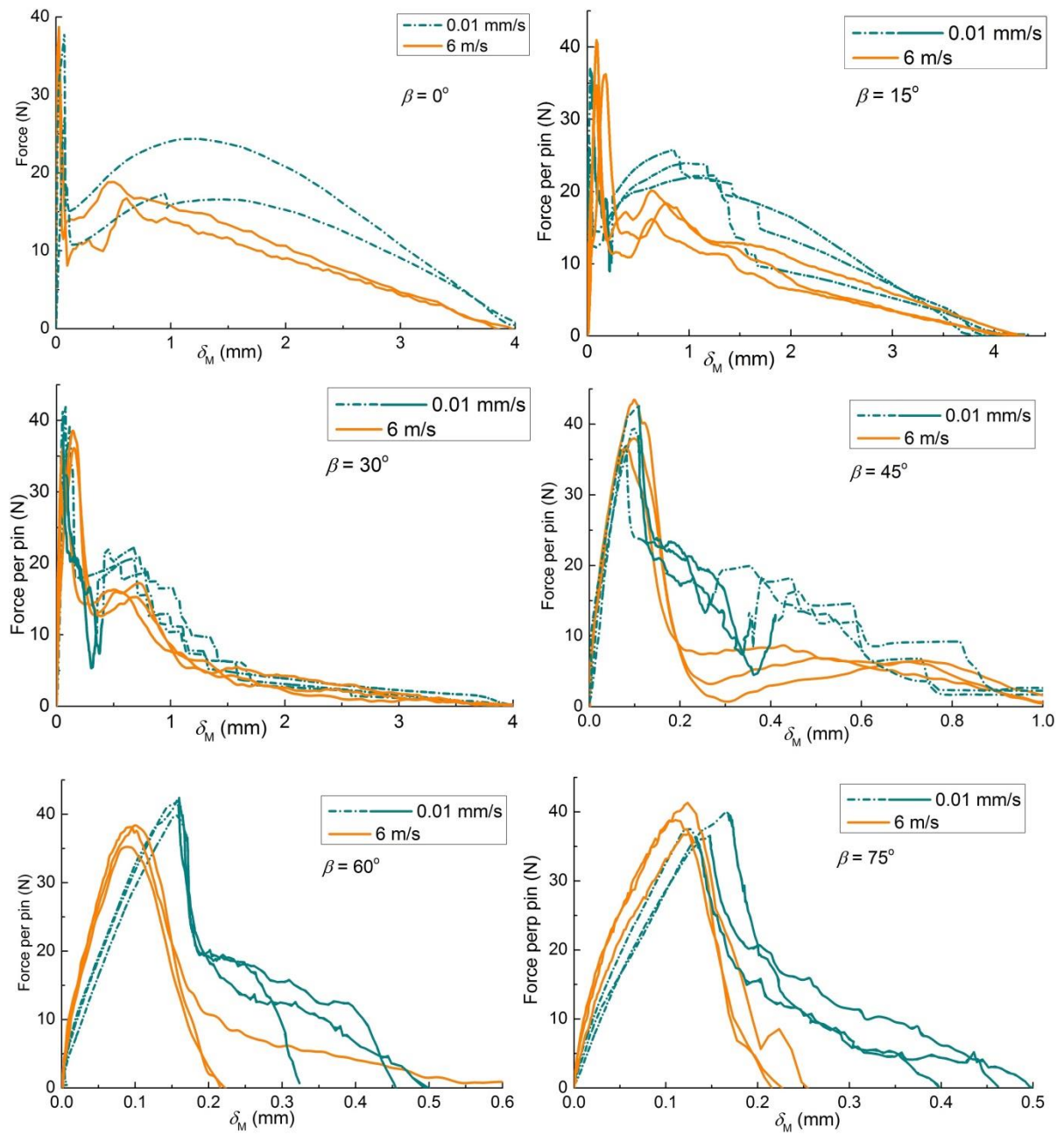


Fig.9. Bridging response at different mode mix angles

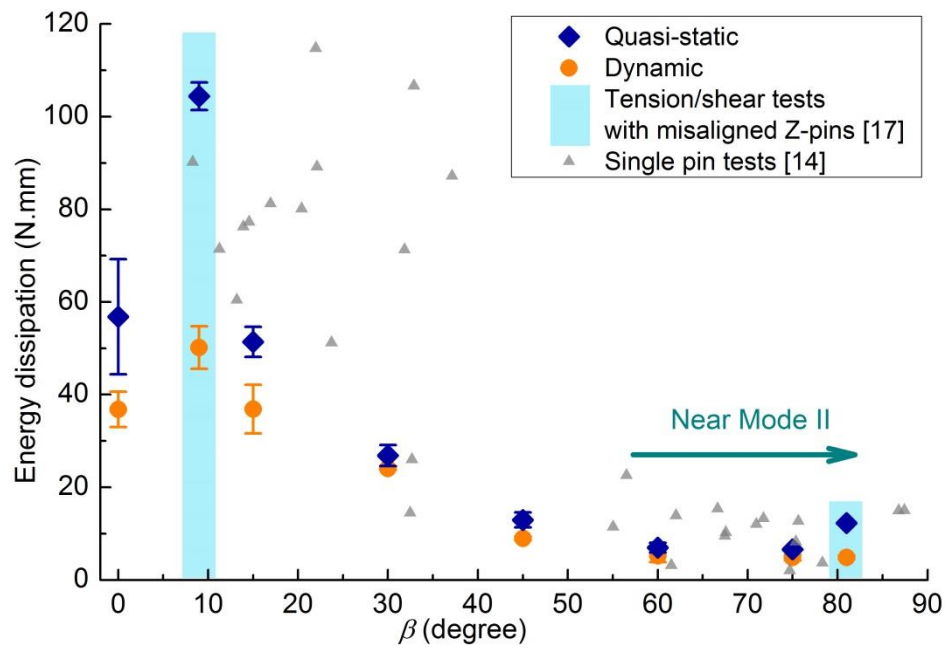


Fig.10 Energy dissipation of individual Z-pins in mixed mode delamination



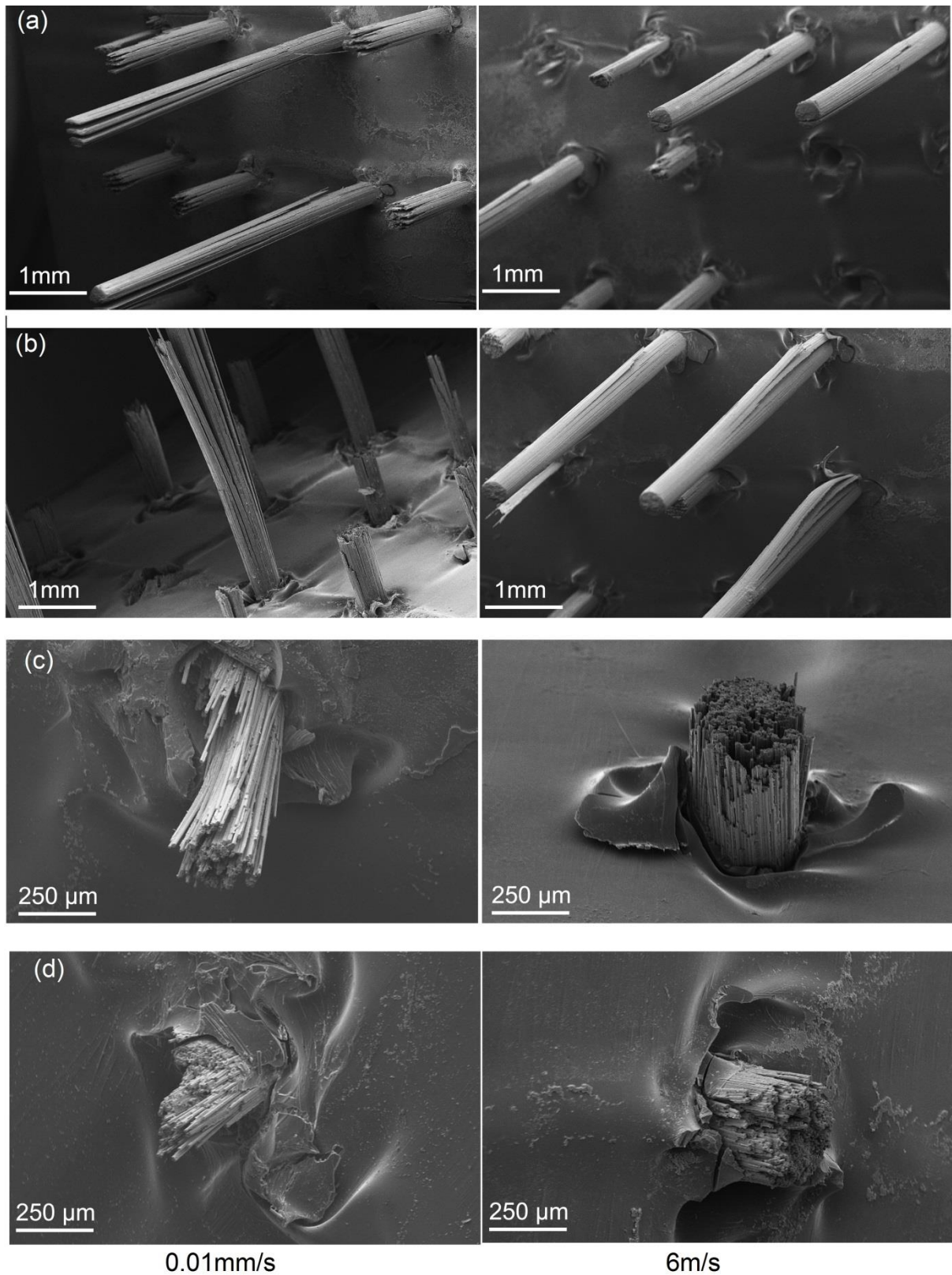


Fig.11 Representative failure modes for Z-pins failed at different loading rate and mixed mode ratios (a)  $\beta=15^\circ$ ; (b)  $\beta=30^\circ$ ; (c)  $\beta=45^\circ$ ; (d)  $\beta=75^\circ$ ;

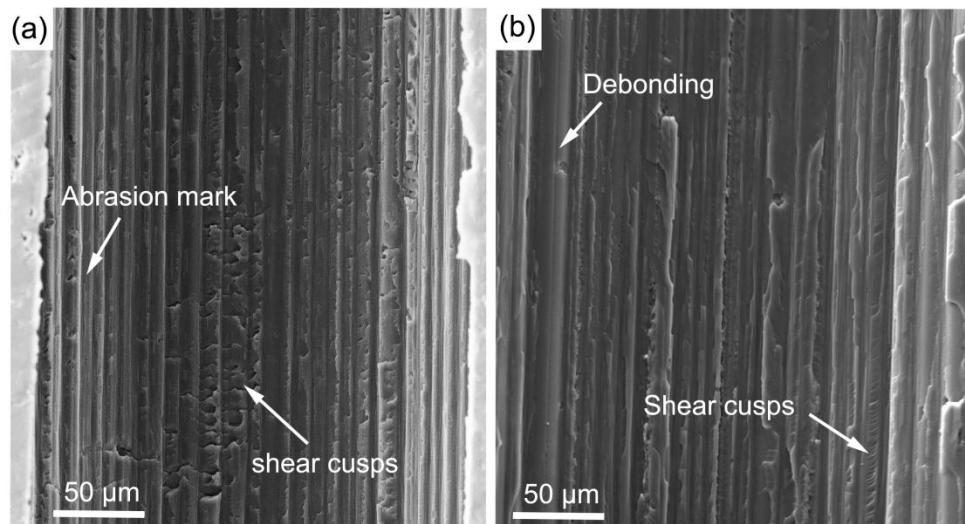


Fig. 12. Failure morphology of pin holes for  $\beta=15^\circ$  from (a) quasi-static and (b) dynamic tests